Available online at www.sciencedirect.com
SCIENCE DIRECT®
Deep-Sea Research I 51 (2004) 653–663
DEEP-SEA RESEARCH
PART I
www.elsevier.com/locate/dsr

Pacific decadal oscillation and sea level in the Japan/East sea

Arnold L. Gordon*, Claudia F. Giulivi

Lamont-Doherty Earth Observatory, Columbia University, Palisades NY 10964, USA

Received 19 March 2003; received in revised form 20 August 2003; accepted 12 February 2004

Abstract

Satellite altimetric data from September 1992 to January 2002 and hydrographic data from 1927 to 1999 reveal the presence of low-frequency variability of sea surface height (SSH) within the Japan/East Sea (JES). SSH interannual variability amounting to approximately 15 cm is in phase with the Pacific Decadal Oscillation (PDO), with higher SSH, warmer, fresher surface (upper 200 dbar) layer during negative phases of the PDO; and lower SSH, cooler, saltier surface layer during a positive PDO. The JES SSH correlation with PDO appears to be related to changes in the geostrophic transport of the Kuroshio, which is weaker during a negative PDO (stronger during positive PDO). The transport of the Tsushima Current, which feeds the JES, is reported to be out of phase with the Kuroshio transport, thus delivering more buoyant subtropical water to the JES when the Kuroshio is weak. Part of the JES baroclinic PDO-related variability may also be due to changes in the freshwater inflow from the East China Sea, which is closely associated with the discharge of the Yangtze River.

1. Introduction

The warm surface waters of the southern Japan/East Sea (JES) are maintained by the import of water through the Tsushima/Korea Strait near 35°N between Japan and Korea (Fig. 1). This warm water, drawn from the East China Sea, is derived from the Taiwan Strait, though some direct feed from a branch of the Kuroshio is likely particularly in autumn (Isobe, 1999). The Tsushima/Korea Strait consists of two channels separated by the Tsushima Island: the eastern channel with a sill depth of 115 m and the western channel with a sill depth of 204 m (Preller and Hogan, 1998). Together they transfer on average 2–3 Sv ($Sv = 10^6\ m^3/s$) of water from the East China Sea into the JES (Inoue et al., 1985; Isoda, 1994; Katoh, 1994; Preller and Hogan, 1998; Isobe et al., 2002), forming the source water of the Tsushima Current within the JES. Measurements from moored ADCP across the Tsushima/Korea Strait from May 1999 to March 2000 revealed a mean transport of 2.7 Sv (standard deviation of 0.9 Sv) with minimum transport in January and maximum in October (Teague et al., 2002). Balancing the Tsushima/Korea Strait inflow are outflows of cold water through the Tsugaru and Soya Straits, the former carrying most of the export. Lee et al. (2000) investigated currents at 15-m depth using 96 Argo tracked surface drifters within the JES. They

*Corresponding author.
E-mail address: agordon@ldeo.columbia.edu (A.L. Gordon).

0967-0637/$ - see front matter
doi:10.1016/j.dsr.2004.02.005

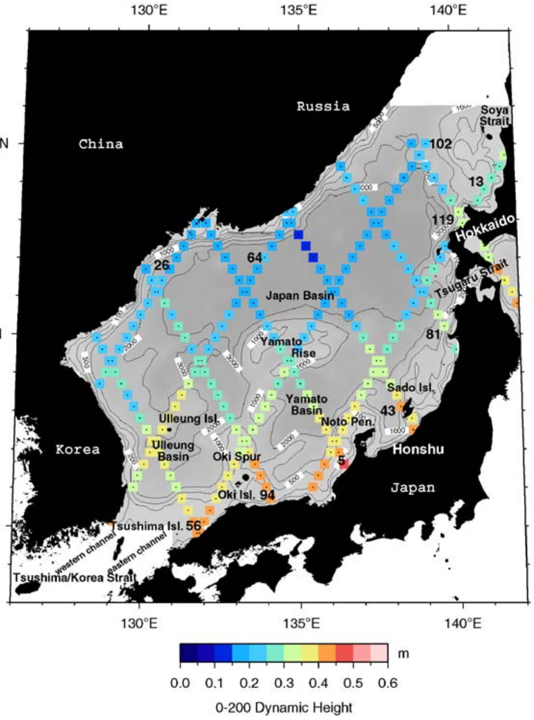

Fig. 1. Mean dynamic height (dynamic meters) map (color) of the sea surface relative to 200 dbar from the hydrographic climatology (from 1927 to 1999) along the *T/P* altimetric data ground tracks every 0.3° of latitude. In the background, contours of the Japan/East Sea bathymetry; isobaths of 100, 200, 500, 1000, 2000 and 3000 m are shown.

found speeds in excess of 40 cm/s to be typical of the Tsushima Current. Drifters entering the JES through the eastern channel tend to follow the Japanese coast, while those entering through the western channel tend to flow along the Korean coast, turning into the interior between 38° and 40°N, marking the subpolar front.

The objective of this work is to investigate the long-term sea level variability within the JES, specifically that associated with the Pacific Decadal Oscillation (PDO), utilizing nearly 9.3 years (September 1992 to January 2002) Pathfinder TOPEX Poseidon (T/P) altimeter data time series and archived JES hydrographic data from 1927 to 1999. Satellite altimeter data have been used in previous studies to investigate eddies and the biennial variability of sea level within the JES basin. Japanese coastal tide gauges have been used to study longer period changes.

Morimoto and Yanagi (2001) mapped monthly sea level data from May 1995 to October 1998. In their EOF analysis, the first mode (87% of the variance) had a maximum amplitude in summer, minimum in winter, which they attributed to variations in the inflow through the Tsushima/Korean Strait. The pattern of the second mode (6% of variance) suggested that it is associated with variability of the various branches of the Tsushima Current.

Hirose and Ostrovskii (2000) using T/P altimeter data from September 1992 to December 1997 found a biennial variability in the sea surface height over the Yamato basin, 37.2–38.6°N, with low-sea level height (SSH) during the summers of 1993, 1995 and 1997 (the latter marginally so). The Yamato Basin feature propagated slowly towards the northwest, inducing low SSH from 39°N to 40°N in the subsequent summers of 1994 and 1996. Shipboard measurements show that the thermocline near 37°N over the Yamato Basin was denser (much cooler and slightly fresher) than normal, when T/P measured low SSH. The same authors, using a reduced gravity model found that the biennial variability might be a JES intrinsic mode response to regional wind forcing.

Senjyu et al. (1999) inspected changes in the JES sea level along both the Japanese and Pacific coasts as recorded by tide gauges from 1956 to 1995. The interannual variability (characterized by the first EOF mode with 46.9% of the variance) occurs simultaneously along all of the Japanese coasts (most pronounced south of 35°N and during the winter months). They attributed this mode to steric effects resulting from winter blasts of cold Asian air masses that occur at peaks of the monsoon index. The second EOF mode (20.8% of the variance) is strongest along the Pacific coast between 136° and 140°E, and it was linked to the meander path of the Kuroshio. The third EOF (15% of the variance) was found to be related to a decadal (20 year) oscillation of which they suggested three possible causes: the 18.6-year nodal tide; vertical displacement of the Japanese Islands and decadal scale changes of the steric height due to water column temperature and salinity changes.

2. Data and methods

Using all available hydrographic data from 1927 to 1999 and T/P altimeter data from September 1992 to January 2002 within the JES, methods were developed to investigate the variability of the sea level. The mean dynamic height of the sea surface relative to 200 dbars (0–200 dbar) was added to the T/P sea surface height anomalies, to obtain absolute sea level. The 200-dbar reference level falls close to the sill depth of the Tsushima/Korean Strait, and marks the base of the thermocline, thus depicting the major part of the baroclinic field (while preserving a relatively high hydrographic station population).

We use NASA/GSFC Pathfinder TOPEX/POSEIDON (T/P) geo-referenced Altimetry Version 9.0 data (Koblinsky et al., 1998) for the period between September 1992 and January 2002 (cycles 1–344), using descending tracks: 56, 94, 5, 43, 81, 119 and ascending tracks: 13, 102, 64, 26 (Fig. 1). These data contain sea surface height anomalies (SSHA) relative to a mean sea level, for 10-day repeat orbit cycles at fixed locations along a reference ground track. Ocean dynamic and range delay corrections were already applied to these data: ocean tide (GOT00.2, ocean tide model, Schrama and Ray, 1996); ionosphere; FMO dry troposphere; FMO inverted barometer (IB); TMR wet troposphere radiometer measurement; solid earth tide (TOPEX SWT algorithm); EM bias (Gaspar MGDR_B Version 2.0 algorithm); Cg center of mass correction; cross track gradient (with respect to CSRMSS95IB); oscillator drift error. Conductivity–temperature–depth (CTD) stations were extracted from the World Ocean Database 2001 (WOD01, Conkright et al., 2002), from 1927 to 1994; Japan Meteorological Agency (JMA) from 1995 to 1997 and from recent cruises by the RV *Revelle*, May–July 1999, and from a RV *Hakuho-Maru* cruise in October 1999.

The along track T/P SSHA were averaged every 0.3° in latitude (approximately 30 km) combining three 10-day cycles and producing monthly sea level anomaly series. To convert T/P SSHA to absolute measures of SSH we have created a long-term sea surface dynamic topography relative to the 200-dbar level for the region of study. The dynamic heights have been computed using all hydrographic measurements available for the region and the climatology was produced by objective analysis (Bretherton et al., 1976; Davis, 1985). The data were interpolated into a 0.3° latitude by 0.3° longitude resolution grid. Quality control of the selected CTD data consisted of comparing temperature–salinity values from individual stations with temperature–salinity values from the entire collection. CTD data were first linearly interpolated to 5 m intervals and then dynamic height relative to 200 dbar was computed for the region resulting in a dataset of 23 651 values, from 1927 to 1999. In order to calculate dynamic height near the ocean boundaries in water shallower than 200 m, the dynamic height profile below the bottom (between 100 and 195 m isobaths) were taken equal to the next profile offshore at the 200 m isobath, assuming no geostrophic shear below the bottom.

3. Results

Three T/P descending tracks: 94, 5 and 43 (Figs. 2a–c) are used to investigate the seasonal and interannual variability of SSH of the central and southern JES. Before presenting the results concerning the PDO signal in the JES, we briefly discuss the seasonal cycle and further evidence of the Yamato Basin biennial variability.

3.1. Seasonal variability of SSH

The SSH seasonal cycle revealed by the three T/P tracks is primarily a response to the steric effects due to the changing water column temperature and salinity (Figs. 2a–c, 3). The spatial and temporal ranges of the 0–200 dbar dynamic height values derived from ship-based hydrographic stations correspond closely with the variability captured by the T/P altimeter data. The mean monthly curves (Fig. 3) show the lowest SSH to occur in late winter, February and March;

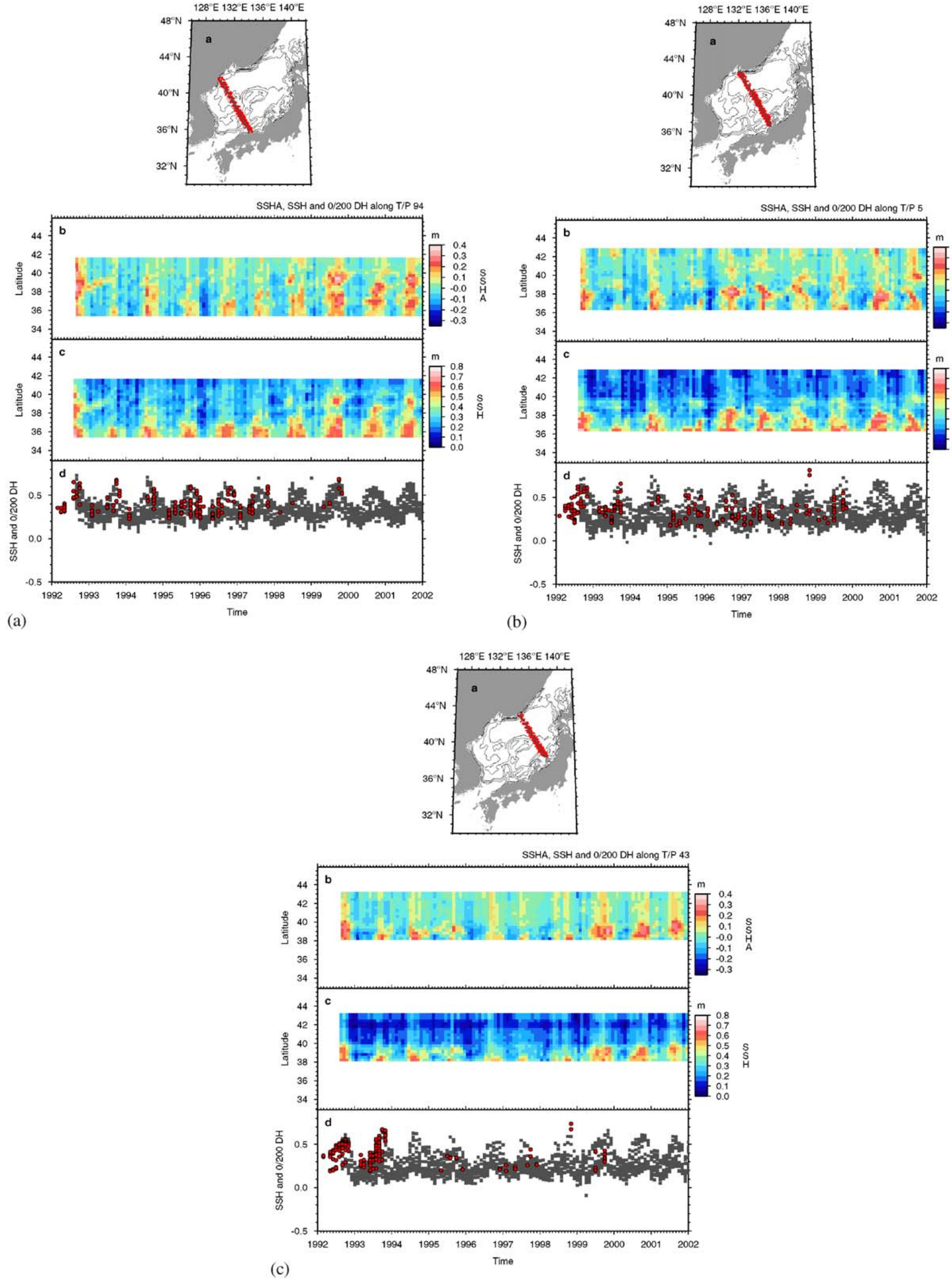

128°E 132°E 136°E 140°E
48°N
44°N
40°N
36°N
32°N
a
SSHA, SSH and 0/200 DH along T/P 94
SSHA, SSH and 0/200 DH along T/P 5
SSHA, SSH and 0/200 DH along T/P 43
b
c
d
Latitude
SSHA
SSH
m
SSH and 0/200 DH
Time
1992
1993
1994
1995
1996
1997
1998
1999
2000
2001
2002
(a)
(b)
(c)

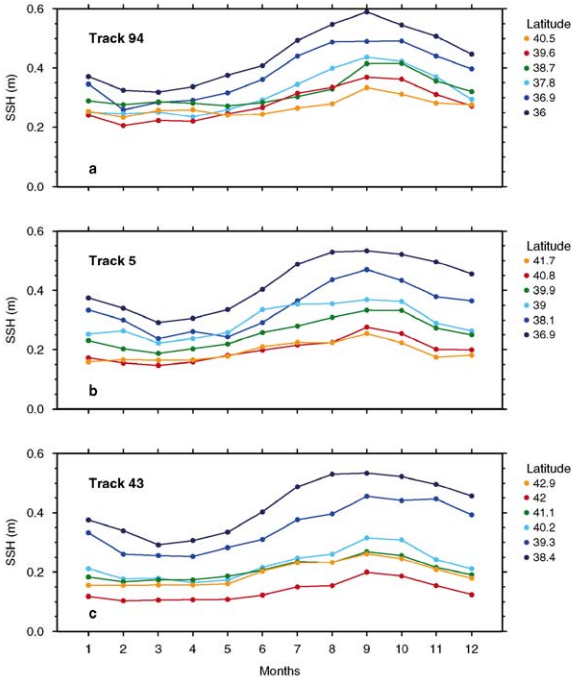

Fig. 3. Monthly variation of the mean SSH (m) along tracks 94 (a), 5 (b) and 43 (c) color-coded for six selected latitudes.

with the highest SSH in late summer, September, lingering into October (Fig. 3). The SSH seasonal range near the coast of Japan is about 0.3 m, while north of the polar front it amounts to only 0.1 m. If the change of 0.3 m is due entirely to thermal expansion, the mean temperature of the upper 200 m would have to change by 9°C. Noting the approximately 10°C sea-surface temperature (SST) range characteristic of the southern JES (see Fig. 3 of Hong et al., 2001) it is reasonable to conclude that the seasonal oscillations of sea level are primarily a thermal effect.

3.2. Interannual variability of SSH

The difference of SSH (Fig. 2) from the mean annual cycle of SSH (Fig. 3) is plotted as δSSH for selected latitudes of the three T/P tracks (Fig. 4). At track 94, the highest δSSH (Fig. 4a) is evident in late 1992 and from 1999 to 2001. Lower δSSH is observed in 1993 and in 1995 to 1996. The periods of 1994, 1997 and 1998 display near zero δSSH. Track 43 (Fig. 4c), while having lower δSSH on average than track 94, shows approximately the

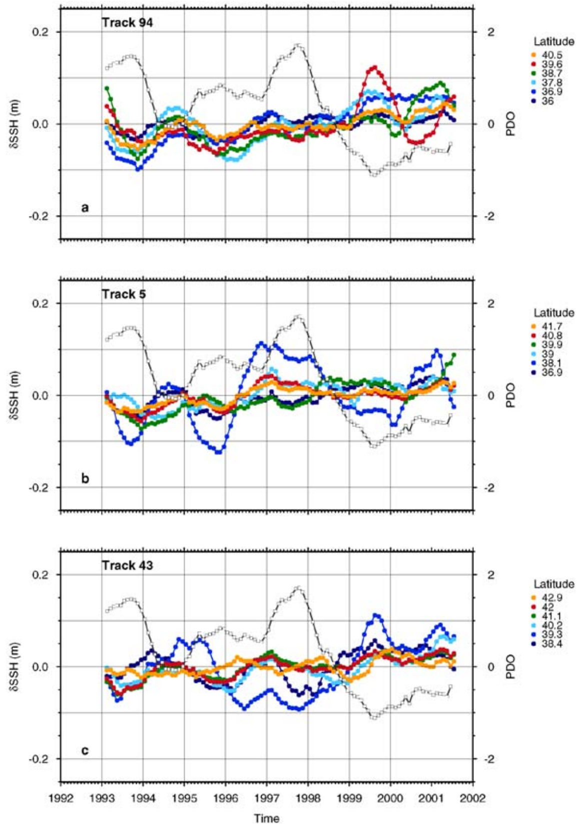

Fig. 4. Time series of SSH anomalies (δSSH) color-coded for selected latitudes. The anomalies are the result of subtracting the long-term monthly curve for each track at selected latitudes (Fig. 3) from each SSH monthly data. Mean (PDO) index shown with a dark line with open squares. All the time series had been filtered with a 12-month running mean.

Fig. 2. (a) Map showing *T/P* data along track 94 (black squares at 30 km intervals) and for comparison, hydrographic stations that fall within ±40 km from a *T/P* location (approximately one Rossby Radius of deformation for the region). (b) SSHA vs. latitude and time from the selected *T/P* track. (c) SSH (SSHA adjusted to the reference dynamic height derived from the hydrographic data) vs. latitude and time from the selected *T/P* track. (d) SSH from the *T/P* data (black squares) and 0–200 dbar dynamic height from CTD (red circles) vs. time along the same track. Figs. 2b and 2c. Same as Fig. 2a but for tracks 5 (2b) and 43 (2c).

same pattern of interannual variability as track 94, with low δSSH in 1993 and 1995, almost zero δSSH in 1994 and from late 1996 to 1998, and high values from 1999 to 2002. However, the interannual variability at track 43, latitude 39.3°N, shows a different behavior. It has a higher amplitude δSSH range and is generally out of phase with the rest of the latitudinal curves, with high δSSH from late 1994 and throughout 1995; low δSSH in 1996–1998, and high δSSH from 1999 to the end of the record in early 2002. At 38.4°N δSSH shows some of this behavior, but to a lesser degree. Track 5 (Fig. 4b) while similar to tracks 94 and 43 displays more variability. Most of the latitudinal curves depict low δSSH values in 1993 and 1995 as do tracks 94 and 43, with near zero δSSH in 1994, but instead of a general δSSH increase in 1999, the increase occurs late in 1996 at latitudes 39.0°N, 40.8°N and 41.7°N, and in 1998 at 36.9° and 39.9°N. The greatest difference occurs at latitude 38.1°N, displaying higher δSSH values in 1996 and 1997.

3.3. Biennial variability

While there is a qualitative relationship between δSSH and PDO (see below) a few points along the tracks 43 and 5 within the Yamato Basin diverge from that relationship. The δSSH of track 5 at 38.1°N displays a much higher degree of variability than those for the rest of the latitudes shown for this particular track (Fig. 4b). The δSSH of track 43 (Fig. 4c) at 39.3°N also reveals this characteristic, though out of phase with that of track 5.

Lee et al. (2000) found a maximum of eddy kinetic energy over the deep Yamato Basin. Morimoto et al. (2000) using T/P and ERS-2 data found that in the Yamato Basin, in an area coinciding with the latitude of 38.1°N of track 5 (Fig. 4b), there was a maximum root mean square (r.m.s.) variability of sea level, which they attributed to regional eddy activity. They found Yamato Basin eddies moving very slowly (1 cm/s) toward the southwest, with lifetimes of 9 months. Morimoto et al. (2000) also found a region of high r.m.s. sea level at the 39.3°N latitude of track 43 (Fig. 4c). They suggested that these features are the same phenomenon as the biennial variability discussed by Hirose and Ostrovski (2000). The 1993 and 1995 low SSH that they discuss agree with the variability of track 5 at 38.1°N, but our study does not reveal the 1997 event, considered by Hirose and Ostrovski (2000) to be of marginal strength. Morimoto and Yanagi (2001) 3rd EOF mode (4% of variance) displays opposite sign between the more energetic feature crossed by track 5 and the one crossed by track 43, which explains the out of phase character of the δSSH found at these two tracks.

Whether due to long-life eddies or the biennial oscillation, it is clear that the sea surface over the deep Yamato Basin, just south of the JES subpolar front behaves somewhat differently than other latitudes crossed by tracks 5 and 43, and may be an internal mode of oscillation of the JES as suggested by Hirose and Ostrovski (2000).

3.4. PDO

T/P tracks 94, 5 and 43 all show high δSSH values in 1992, low δSSH in 1993 and 1995, near zero δSSH in 1994, 1997 and into 1998, and high δSSH from late 1998 to the end of the T/P records in early 2002. After removal of the Yamato Basin SSH anomalous data points of track 5 and 43 and the seasonal cycle, there is a relationship, particularly south of the polar front (correlation coefficient is 0.4 at the 95% confidence level), between PDO and δSSH within the JES (Fig. 4): sea level is higher during a negative PDO, lower during a positive PDO. To investigate the decadal variability of the sea level and its relationship with PDO, we inspect the longer record offered by the hydrographic data.

The 5-year running mean sea surface dynamic height relative to 200 dbar within the station grid for the period 1927–1999 (Fig. 5; the station grid is positioned south of the polar front in a region with lower variability and where better correlations were found) supports the relationship with PDO. Clearly other factors are at play, but the PDO imprint is apparent, with high sea level during the negative PDO events around 1950 and 1974, with low sea level in the 1930s and during the positive or rising PDO of the 1980s. The relationship

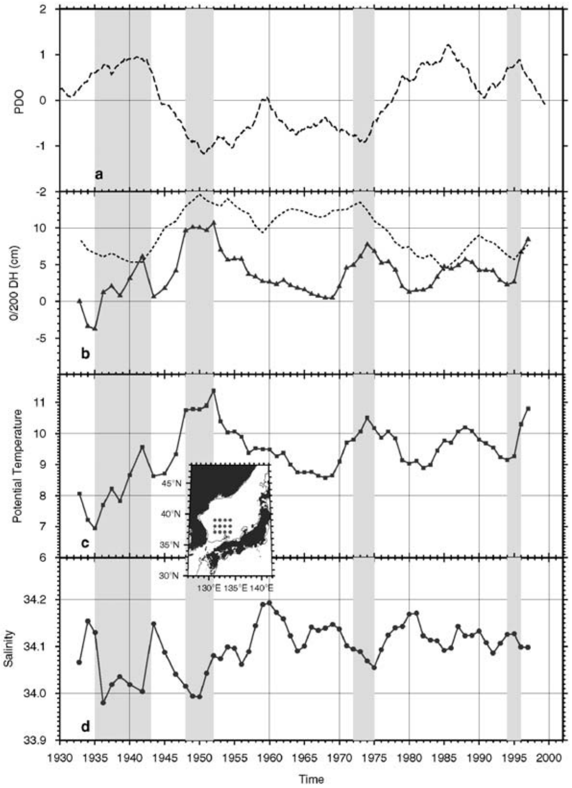

Fig. 5. (a) Time series of Pacific Decadal Oscillation Index (PDO), (b) 0 and 200 dbar dynamic height (black line with triangles) and the predicted dynamic height (dashed line) based on a linear relation with PDO, (c) temperature and (d) salinity of the upper 200 m of selected hydrographic stations shown in the map inset. A 5-year running average was applied to the series. The gray vertical bars in the background identify periods of better correlation between 0 and 200 dbar and PDO: 1935–1943; 1948–1952 and 1972–1975.

appears to decrease somewhat in the later decades. At the 95% confidence level, from 1927 to 1960 the correlation coefficient is 0.6; from 1927 to 1980 it is 0.5; and for the entire record it is 0.3. The comparison of the observed 0–200 dbar sea surface dynamic height with the 0–200 dbar based on a linear relation to the PDO shows that there are specific periods where the observed 0–200 dbar deviates from the PDO, such as from the late 1950s to early 1960s and then from the late 1970s to mid1980s.

Inspection of the temperature and salinity of the upper 200 m (which includes most of the thermocline and hence major part of the baroclinic mode) shows a close relationship to temperature: warmer when sea level is high (negative PDO), colder, when sea level is low (positive PDO). The temperature range for the upper 200 m is about 4°C. Additionally, there is an inverse relationship with salinity: saltier water during the cooler phase, fresher water during the warmer phase. The salinity range amounts to about 0.2. Both temperature and salinity act together to produce the steric change, with temperature being the dominant variable, accounting for two thirds of the sea surface variability.

4. Discussion

The JES baroclinic sea level has variations correlated with the PDO. The PDO is primarily a mid-latitude Pacific sea surface temperature index and is similar to the sea level air pressure (see Fig. 7.3.2 of Dickson et al. (2001) for the North Pacific index from 1925 to 1998; Figs. 3, 4 of Mantua et al., 1997; Talley et al., 2001, see their Fig. 7.1.3 for the PDO time series from 1940 to 2000; Seager et al., 2001; see: http://tao.atmos.washington.edu/pdo/). Negative PDO regimes prevailed from 1890 to 1924 and again from 1947 to 1976, while positive PDO phases dominated from 1925 to 1946 and from late 1976 through most of the 1990s. Trenberth and Hurrell (1994) refer to the 1976 event as the time of a major climate regime shift. Inspection of the PDO annual average (Fig. 7.1.3 of Talley et al., 2001) reveals that 1992 marks the end of a short negative PDO phase extending from 1989 to 1992. The PDO is positive until mid1998, with a brief period of near zero PDO in 1994, becoming negative from mid1998 to 2002. During the positive phase, the Aleutian Low becomes deeper and shifts to the south and the westerlies over the North Pacific strengthen. This causes an increased southward Ekman transport leading to lower SST at mid-latitudes. The southward shift of the zero wind stress curl eventually causes the Kuroshio to separate from the coast of Japan at a more southern latitude, reinforcing a cool mid-latitude SST (Seager et al., 2001).

One hypothesis may be that changes in the Kuroshio geostrophic transport reflects variations of the sea level difference between the JES and the subtropical North Pacific. Kawabe (1995), using tide gauge data, provided a 1957–1992 time series of Kuroshio transport. His series shows a low transport prior to 1975 and higher after 1975. Repeated hydrographic sections south of Japan along 135°15'E had been used to produce a 1955–1997 time series of Kuroshio transport (geostrophic relative to 1000 dbar; Nakamura and Hinata, 1999; Dickson et al., 2001, their Fig. 7.3.12). It shows high transport in the mid1960s, minimum in 1975, and increasing transport (with local dips and peaks) to the mid1980s staying relatively high to the end of the record. Comparison of the Kuroshio with the PDO suggests that its transport is large (large sea level slope across the current) with a positive PDO, small (reduced sea level slope across the current) with a negative PDO. This is consistent with the hypothesis: low JES SSH for strong Kuroshio. While the slope change may be associated with sea level change on either side of the Kuroshio, our study suggests that we may expect at least some of the sea level change occurs within the JES.

Nitani (1972; his Fig. 29) found that the transport of the Tsushima Current and Osumi branch (the Osumi branch is a minor component which flows along the Pacific coast of Japan immediately to the east of the Tsushima/Korean Strait entrance) of the Kuroshio from 1955 to 1965 is inversely related to the Kuroshio transport. A weaker Kuroshio would therefore deliver to the JES, via the Tsushima/Korean Strait, an increased amount of buoyant subtropical water, thus accounting for higher SSH during a negative PDO. Shaw and Wyrtki (1972) model suggests a simple concept that may account for the Tsushima and Kuroshio relationship. Assuming that the volume of warm water within the subtropical thermocline remains constant, relaxed transport of the western boundary current would force an expansion of the surface areal extent of the subtropical gyre, which would increase the inflow of subtropical water to the JES.

Casey and Adamec (2002) with Pathfinder SST and T/P data inspected the SST and SSH variability over the entire North Pacific from 1993 to late 1999. They found that the highest correlations of these parameters occur at low latitudes with ENSO (El Niño-southern oscillation index), but at the subtropical western North Pacific (north of 20°N, see their Fig. 7) there is a correlation with PDO, with higher SST and SSH when PDO is positive. A one month lag of SSH to PDO is suggested. The JES is not well resolved by their large area treatment. Their research indicated that some of the Kuroshio transport change is due to the subtropical Pacific SSH change.

The hydrographic data (Fig. 5) indicate the baroclinic nature of the response: the upper 200 dbar is warmer, fresher when PDO is negative. Changes in the JES steric sea level are due to changes in the water column heat and freshwater induced by local sea-air fluxes or by buoyancy transport through the Tsushima/Korean Strait. While it is difficult to separate these two factors, there is some indication that variations of the inflow temperature and salinity are involved: (1) The inverse transport relationship between the Kuroshio and the Tsushima Current (Nitani, 1972) as mentioned above and (2) the river inflow to the East China and Yellow Seas. Our results are consistent with Isobe (1999) and Isobe et al. (2002) thoughts, that the water that forms the Tsushima Current is modified by the water exchange with the Kuroshio and by the East China and Yellow Seas.

The flow through the Tsushima/Korean Strait carries all of the freshwater introduced by rivers into the Yellow and East China Seas (Isobe et al., 2002). The discharge of the largest of these rivers, the Yangtze and Yellow River (the Yangtze being by far the largest) fluctuates with PDO; with high runoff (low) when PDO is negative (positive; the 5-year running mean is shown in Fig. 6). The residual after the linear trend of the Yangtze runoff is removed (the Yangtze at the gauging stations shown in Fig. 6a, has decreased slightly during the course of the 20th century; Fig. 6b), more clearly shows the correlation with PDO. While there is some variability by a few years in terms of phase between the runoff and PDO, a relationship is evident. An exception to this rule is the runoff peak in the early 1970s, though PDO has a negative tendency. It is suspected that other

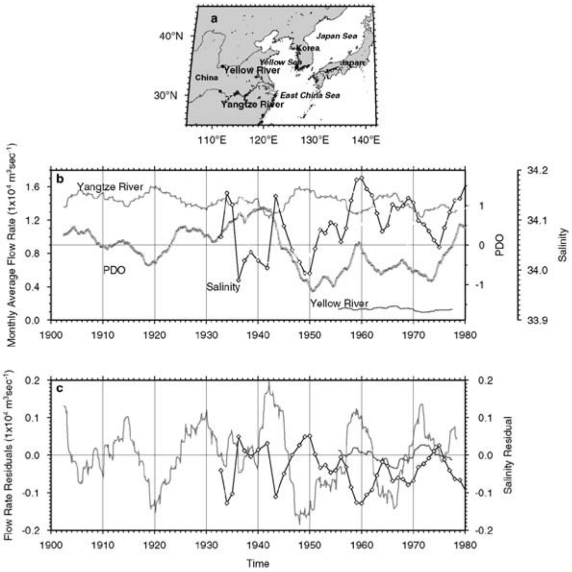

Fig. 6. (a) Map showing the location of the runoff gauging stations used in this study. (b) Time series of the 5-year running averaged Yangtze River and Yellow River flow rates ($m^3 s^{-1} \times 10^4$), PDO and salinity from the area shown in the inset map of Fig. 5. (c) Flow rate and salinity residuals vs. time. The residuals were obtained after subtracting the linear trend from each series. The monthly average runoff was extracted from NASA ISLSCP GDSLAM Hydrology-Soils global data sets available at http://www.ingrid.ldeo.columbia.edu.

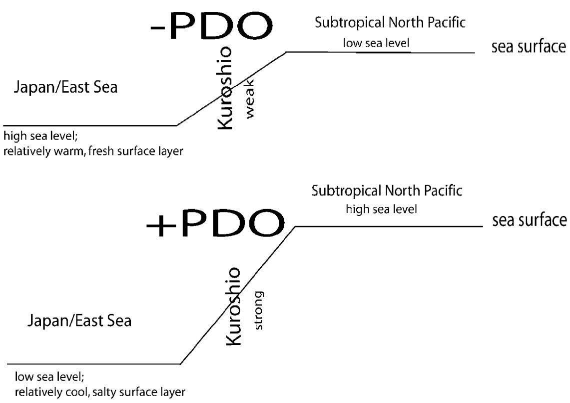

Fig. 7. A schematic representation of the changes of sea level and Japan/East Sea surface layer temperature and salinity associated with positive and negative phases of the PDO.

climate phenomena contribute to the precipitation in the Yangtze basin, such as ENSO and monsoon events, but the PDO signature is present. Presumably higher freshwater inflow into the East China Sea and JES leads to a more stratified surface layer, in which summer warming would be concentrated.

5. Conclusions

The difference of sea surface height (SSH) from the mean annual cycle of SSH (δSSH) within the Japan/East Sea (JES) as detected by TOPEX/Poseidon (T/P) altimeter during the period September 1992 to January 2002, displays significant interannual variability, with an amplitude of approximately 15 cm, similar to the sea surface dynamic height variability relative to the 200 dbar level observed by the hydrographic data set from 1927 to 1999. The JES sea height low frequency variability correlates with the PDO index: higher SSH with warmer, fresher surface layer water during negative phases of PDO; and lower SSH with cooler, saltier surface layer during a positive PDO (Fig. 7). After a long period of negative PDO, beginning in 1940, a positive PDO has been dominant since 1976, though periods of near zero PDO have occurred, such as in the early 1990s. However in late 1998, PDO appears to have switched to a negative phase, remaining negative to the end of the altimeter record used in this study.

It is proposed that the JES δSSH correlation with PDO is due to changes in the Kuroshio geostrophic transport, which is weaker during a negative PDO (stronger during a positive PDO). This relationship may be a consequence of the inverse relationship between the Tsushima Current transport and that of the Kuroshio. As the Kuroshio weakens (strengthen) the injection of buoyant North Pacific subtropical water into the JES via the Tsushima/Korean Strait increases (decreases). Another source of the JES SSH baroclinic variability may be coupled to changes in the freshwater inflow from the East China Sea, which is associated with the discharge of the Yangtze River. Changes in the Yangtze runoff due to damming will have an effect on JES sea level, in addition to ventilation (Nof, 2001).

Acknowledgements

We thank an anonymous reviewer whose constructive comments led to a far improved study. The Office of Naval Research, special program on the Japan/East Seas, Grant N00014-99-1-0092, supported the research presented in this paper. We appreciate the efforts of the NASA Ocean Altimeter Pathfinder Project and the programming support of Phil Mele, Lamont-Doherty Earth Observatory Contribution Number 6575.

References

Bretherton, F.P., Davis, R.E., Fandry, C.B., 1976. A technique for objective analysis and design of oceanographic experiments applied to MODE-73. Deep Sea Research 23, 559–582.

Casey, K.S., Adamec, D., 2002. Sea surface temperature and sea surface height variability in the North Pacific Ocean from 1993 to 1999. Journal of Geophysical Research 107(C8), 10.1029/2001JC001060.

Conkright, M.E., Antonov, J.I., Baranova, O., Boyer, T.P., Garcia, H.E., Gelfeld, R., Johnson, D.D., Locarnini, R.A., Murphy, P.P., O'Brien, T.D., Smolyar, I., Stephens, C., 2002. World Ocean Database 2001, Volume 1: Introduction. In: Levitus, S. (Ed.), NOAA Atlas, NESDIS 42. US Government Printing Office, Washington, DC, pp. 167.

Davis, R.E., 1985. Drifter observations of coastal surface currents during CODE: the statistical and dynamical views. Journal of Geophysical Research 90, 4576–4772.

Dickson, B., Hurrell, J., Bindoff, N., Wong, A., Arbic, B., Owens, B., Imawaki, S., Yashayaev, I., 2001. The World during WOCE 2001. The WOCE Synthesis. In: Siedler, G., Church, J. (Eds.), Ocean Circulation and Climate. International Geophysics Series. Academic Press, New York, pp. 557–583.

Hirose, N., Ostrovskii, A.G., 2000. Quasi-biennial variability in the Japan Sea. Journal of Geophysical Research 105 (C6), 14011–14027.

Hong, C.-H., Cho, K.-D., Kim, H.-J., 2001. The relationship between ENSO events and sea surface temperature in the East (Japan) Sea. Progress in Oceanography 49, 21–40.

Inoue, N., Miita, T., Tawara, S., 1985. Tsushima Strait II: physics. In: Kunishi, H., et al. (Ed.), Coastal Oceanography of Japanese Islands. Tokai University Press, Tokyo, pp. 914–933.

Isobe, A., 1999. On the origin of the Tsushima Warm Current and its seasonality. Continental Shelf Research 19 (1), 117–133.

Isobe, A., Ando, M., Watanabe, T., Senjyu, T., Sugihara, S., Manda, A., 2002. Freshwater and temperature transports through the Tsushima/Korea Straits. Journal of Geophysical Research 107(C7), 10.1029/2000JC000702.

Isoda, Y., 1994. Warm eddy movements in the Eastern Japan/East Sea. Journal of Oceanography 49, 443–458.

Japan Meteorological Agency (JMA), Oceanographical Division, Climate and Marine Department, CD-ROM 1995,1996,1997.

Katoh, O., 1994. Structure of the Tsushima Current in the Southwestern Japan/East Sea. Journal of Oceanography 50, 317–338.

Kawabe, M., 1995. Variations of the current path, velocity and volume transport of the Kuroshio in relation with the large meander. Journal of Physical Oceanography 25 (12), 3103–3117.

Koblinsky, C.J, Ray, R.D., Beckley, B.D., Wang, Y.M., Tsaoussi, L., Brenner, A.C., Williamson, R.G., 1998. NASA Ocean Altimeter Pathfinder Project Report 1: Data Processing Handbook. NASA Technical Memorandum NASA/TM-1998-208605.

Lee, D.-K., Niiler, P., Lee, S.-R., Kim, K., Lie, H.-J., 2000. Energetics of the surface circulation of the Japan/East Sea. Journal of Geophysical Research 105 (C8), 19561–19573.

Mantua, N.J., Hare, S.R., Zhang, Y., Wallace, J.M., Francis, R.C., 1997. A Pacific decadal climate oscillation with impacts on salmon. Bulletin of the American Meteorological Society 78, 1069–1079 Morimoto, A., Yanagi, T., 2001. Variability of sea surface circulation in the Japan Sea. Journal of Oceanography 57 (1), 1–13.

Morimoto, A., Yanagi, T., 2001. Variability of sea surface circulation in the Japan Sea. Journal of Oceanography 57 (1), 1–13.

Morimoto, A., Yanagi, T., Kaneko, A., 2000. Eddy field in the Japan Sea derived from satellite altimetric data. Journal of Oceanography 56, 449–462.

Nakamura, T., Hinata, T., 1999. Seasonal and interannual variations of the Kuroshio south of Japan. Weather Service Bulletin 66 (special issue), S33–S41.

Nitani, H., 1972. Beginning of the Kuroshio. In: Stommel, H., Yoshida, K. (Eds.), Kuroshio Physical Aspects of the Japan Current University of Washington Press, pp. 129–163.

Nof, D., 2001. China's development could lead to bottom water formation in the Japan/East Sea. Bulletin of the American Meteorological Society 82 (4), 609–618.

Preller, R.H., Hogan, P.J., 1998. Oceanography of the Sea of Okhotsk and the Japan/East Sea. In: Robinson, A., Brink, K. (Eds.), The Sea, Vol. 11. Wiley, New York, pp. 429–481 (Chapter 15).

Seager, R., Kushnir, Y., Naik, N.H., Cane, M.A., Miller, J., 2001. Wind-driven shifts in the latitude of the Kuroshio–Oyashio extension and generation of SST anomalies on decadal timescales. Journal of Climate 14 (22), 4249–4265.

Senjyu, T., Matsuyama, M., Matsubara, N., 1999. Interannual and decadal sea-level variations along the Japanese coast. Journal of Oceanography 55, 619–633.

Shaw, R., Wyrtki, K., 1972. The shape of the warm surface layer in a subtropical gyre. In: Gordon, A.L. (Ed.), Studies in Physical Oceanography—A Tribute to George Wust on

His 80th Birthday, Vols. 1 and 2. Gordon and Breach, New York, Science Publ., N.Y., pp. 179–194.

Talley, L.D., Stammer, D., Fukumori, I., 2001. The WOCE synthesis. In: Siedler, G., Church, J. (Eds.), Ocean Circulation and Climate. International Geophysics Series. Academic Press, New York, pp. 525–546.

Teague, W., Jacobs, G., Perkins, H., Book, J., Chang, K.-I., Suk, M.-S., 2002. Low-frequency current observations in the Korea/Tsushima Strait. Journal of Physical Oceanography 32 (6), 1621–1641.

Trenberth, K.E., Hurrell, J.W., 1994. Decadal atmospheric–ocean variations in the pacific. Climate Dynamics 9, 303–319.